

Preparation and Application of Dual-Crosslinked Compressible Expandable Aerogel Dressing

Abu Bari ^{1,*}, Rahman Akter ¹

¹ Department of Textile Engineering, Dhaka University of Engineering & Technology, Gazipur 1707, Bangladesh

*Corresponding author: A.Bari@duet.ac.bd

Abstract. Medical dressings are critical materials for wound care, effectively promoting wound healing and alleviating patient suffering. With social development and improved living standards, higher functional requirements for medical dressings have emerged. In areas such as sensitive wound care and cavity bleeding, elastic and expandable dressings play vital roles. Aerogel dressings, characterized by their three-dimensional porous structure, low density, high porosity, and high specific surface area, offer significant advantages. Currently, polyurethane aerogels are the most commonly used functional aerogel dressings. However, their preparation heavily relies on petroleum-derived chemicals such as methylene diphenyl diisocyanate and toluene diisocyanate, resulting in high production costs, high prices, and poor degradability, which limit their widespread application. Natural polymers, as important biomass materials, offer advantages such as wide availability, excellent biocompatibility, and soil degradability. Amidst increasing petroleum resource shortages and environmental concerns, it is urgent to develop natural polymer aerogel dressings with tailored structures and properties to achieve green iterative upgrades of functional aerogel dressings. This study utilizes sodium carboxymethyl cellulose (CMC), hydroxypropyl cellulose (HPC), and coniferous pulp (CP) as raw materials. Through dual physical and chemical crosslinking strategies, combined with ice-templating, pore-forming agents, and foaming agents, a multi-level porous structure was constructed to prepare CMC-CP dual-crosslinked compressible expandable aerogel dressings. The structure and properties of the resulting aerogel dressings were tested and analyzed. The results indicate that heating promotes glutaraldehyde (GA) to form covalent bonds between CMC and CP, achieving chemical crosslinking. The introduction of HCl protonates the sodium carboxylate groups of CMC into carboxyl groups. Using a foaming agent (SDS), the mixture is fully foamed. Freezing facilitates hydrogen bonding for physical crosslinking and leverages the synergistic pore-forming effects of the foaming agent and ice-templating. After freeze-drying, an aerogel dressing with a hierarchical porous structure is obtained. The CMC-CP dual-crosslinked compressible expandable aerogel dressing exhibits high strength, excellent compressibility, and liquid-absorption expansion properties. Compared to gelatin sponges and medical gauze, the aerogel dressing demonstrates good in vitro cytocompatibility, indicating its promising application potential and practical value as a wound dressing.

Keywords: *Sodium carboxymethyl cellulose; Hydroxypropyl cellulose; Coniferous pulp; Dual-crosslinking; Aerogel dressing*

Received on 01 March 2024, Accepted on 18 May 2024, Published on 15 Junly 2024

Copyright © 2024 Abu Bari *et al.* licensed to JGEEE. This is an open access article distributed under the terms of the CC BY-NC-SA 4.0, which permits copying, redistributing, remixing, transformation, and building upon the material in any medium so long as the original work is properly cited.

1 Introduction

Aerogels represent a class of lightweight solid materials featuring a three-dimensional porous network structure with gas as the dispersed phase, typically exhibiting porosity exceeding 90% [1-2]. These materials possess extremely low density – sometimes approaching only three times that of air – while maintaining structural integrity under mechanical stress. Since the initial successful preparation of silica aerogel in 1931 by Kistler [3], research on aerogel materials has experienced continuous development. Breakthroughs in manufacturing

technologies, particularly sol-gel processes and ambient pressure drying methods, have significantly improved production efficiency while substantially reducing costs, enabling the transition of aerogel materials from laboratory research to practical applications across various fields including medical technology, aerospace engineering, construction industries, energy sectors, and environmental protection [4-7].

In recent years, aerogel materials have emerged as significant components in the biomedical materials domain, with new application cases continually emerging. Medical dressings, as essential healthcare materials, must satisfy multiple critical criteria: Firstly, dressing materials must provide complete and effective wound coverage while maintaining appropriate moisture levels to facilitate cellular growth and proliferation. Secondly, these materials need to ensure adequate permeability to water vapor and gases, creating a comfortable and stable microenvironment conducive to wound healing. Thirdly, dressing materials should possess suitable adhesion characteristics and sufficient mechanical properties to maintain effective wound coverage without causing patient discomfort during movement. Fourthly, antibacterial functionality is essential to prevent wound infection complications. Fifthly, excellent biocompatibility is mandatory to avoid adverse effects on patient health.

Aerogel materials, with their inherent low-density three-dimensional porous structure and considerable structural strength, guarantee excellent moisture absorption and retention capabilities while providing optimal breathability. These characteristics create an ideal framework for cell adhesion and tissue regeneration, thereby accelerating wound healing processes. With advancing research on natural polymers and their derivatives, the elasticity, antibacterial properties, and biocompatibility of aerogel materials have shown remarkable improvement [8-10]. Consequently, the superior characteristics of aerogel materials can effectively address multiple requirements of modern wound dressings. Composite medical dressings utilizing aerogel materials as the core functional layer (hereinafter referred to as aerogel dressings) demonstrate advantages that traditional dressings cannot match, attracting considerable attention from researchers worldwide.

The international market has recently witnessed the emergence of innovative hemostatic dressing materials, notably the X-stat hemostatic device developed by ReviveSurgical (USA). This novel hemostatic material, manufactured from synthetic polymer particles, exhibits exceptional performance in rapidly controlling severe external hemorrhage, finding extensive applications in battlefield medicine and emergency surgical situations. The X-stat material presents as compressed small cotton-like sheets that are injected into wounds using a specialized applicator device. Upon contact with blood, these sheets rapidly absorb fluid and expand 8-12 times within seconds to fill the wound cavity, creating mechanical pressure that promotes wound channel closure and prevents further blood loss.

This research aims to develop a hemostatic dressing with functionality comparable to the X-stat device. CMC, as an etherified cellulose derivative, offers excellent water solubility and outstanding biocompatibility. CP, consisting of wood fiber pulp derived from coniferous trees through chemical or mechanical processes, provides high mechanical strength and remarkable stiffness, significantly enhancing the overall structural integrity of the aerogel dressing. Therefore, these materials were selected as primary components for fabricating compressible expandable hemostatic dressings.

This study employs CMC and CP as raw materials, introducing GA as a chemical crosslinking agent [11-12]. Through the establishment of dual physico-chemical crosslinking networks involving both covalent and hydrogen bonds, CP is effectively incorporated into the CMC hydrogen-bonded network, imparting dual-crosslinking characteristics to the aerogel dressing. The synergistic application of ice-templating methodology and SDS foaming agent enables the construction of a hierarchical porous structure in the compressible expandable aerogel dressing. The ultimate outcome is the successful preparation of CMC-CP dual-crosslinked compressible expandable aerogel dressings, with systematic investigation of critical factors influencing the dressing's performance characteristics.

2 Materials and methods

2.1 Preparation of CMC-CP Dual-Crosslinked Compressible Expandable Aerogel Dressing

The experimental procedure utilized CMC and CP as primary raw materials. Hydrochloric acid was introduced to create an acidic environment, facilitating the formation of hydrogen bond networks between CMC and CP to achieve physical crosslinking. Glutaraldehyde served as the chemical crosslinking agent to establish covalent bonds between CMC and CP molecules, realizing chemical crosslinking. The final CMC-CP compressible expandable aerogel dressing was obtained through ice-templating methodology followed by freeze-drying processing. To prevent excessive viscosity that could compromise processability, the CMC content was maintained below 4% while CP content was controlled under 2% in the final formulation.

Specific quantities of CMC (0.1, 0.2, 0.3, 0.4 g) and CP (0.2 g) were added to deionized water to prepare a homogeneous mixture with total mass of 10.0 g. The mixture was vigorously stirred to ensure uniform distribution of CP fibers throughout the solution. Subsequently, 2.0 mL of HCl solution (20.0 wt%) and 1.0 mL of GA solution (1.0 wt%) were added to the mixture, followed by stirring at 700 rpm for thorough homogenization. Then, 1.0 mL of SDS solution (0.5 wt%) was introduced with intensive stirring to achieve optimal foaming effects. The resulting foam was carefully transferred into a syringe and injected into centrifuge tubes, followed by centrifugation at 500 rpm to remove oversized bubbles. The samples were subsequently heated at 70°C for 3 hours to promote chemical crosslinking reactions.

After the heating process, samples were cooled to room temperature and transferred to a -16°C freezer for 24 hours to facilitate low-temperature crosslinking and implement the first ice-templating cycle. Following complete thawing, the hydrogels were thoroughly washed with deionized water to eliminate residual HCl, GA, and SDS compounds, ultimately yielding CMC-CP dual-crosslinked hydrogel precursors.

2.2 Characterization and Testing Methods

2.2.1 Density Measurement

Use a spiral micrometer to measure the dimensions of the sample multiple times (at least 3 times) and calculate the volume of the sample. Use an electronic balance to measure the sample mass multiple times (weighing at least 3 times), and use the above data to calculate the sample density.

2.2.2 Morphological Observation

The aerogel dressing was observed by Zeiss Sigma 360 field emission scanning electron microscope with conventional test voltage of 10.0-15.0 kV. In order to obtain better test results, it is necessary to improve the conductivity of the sample. Therefore, a gold spraying instrument is used to spray the sample for a duration of 180 seconds.

2.2.3 FT-IR Analysis

Use the Nicolet iS50 FT-IR spectrometer produced by Thermo Fisher in the United States, with a conventional testing range of 4000-400 cm⁻¹, to analyze the molecular structure and functional group information of the sample and its raw materials. Before testing, the sample to be tested needs to be dried to thoroughly remove any moisture from the sample.

2.2.4 Specific Surface Area Measurement

Micromeritics ASAP 2460 surface area analyzer was used to test the N₂ adsorption/desorption characteristics of aerogel, and BET model was used to calculate its specific surface area. Before the test, the sample is degassed at 110 °C for 12 h to eliminate the small molecules remaining in the gel. Type III isotherms are used to calculate the specific surface area of aerogels. Before testing, the sample needs to be dried to remove moisture from the sample.

2.2.5 Liquid Absorption Capacity

The absorption energy of PU dressing, CMC-HPC double crosslinked high elastic aerogel dressing and CMC-CP double crosslinked compressed inflation gas gel dressing to simulated blood and simulated body fluid was measured by the method described in the pharmaceutical industry standard Test Methods for Contact Wound Dressing Part 1: Liquid Absorption. Cut the sample into a size of 2 cm × 2 cm and immerse it completely in a culture dish containing simulated blood and a culture dish containing simulated body fluid for 0.5 hours. Maintain the experimental temperature at normal human body temperature (set at 37 °C here). When weighing, use tweezers to pick up a corner of the sample and suspend it above the culture dish. After there are no liquid droplets, place it on an electronic balance for weighing. Remove the maximum and minimum values from the test results of each dressing group, and calculate the final result by averaging the remaining results.

2.2.6 Water Vapor Permeability

The water vapor permeability of PU dressings, CMC-HPC double crosslinked high elastic aerogel dressings and CMC-CP double crosslinked compressed swelling gas gel dressings was measured by the method specified in the pharmaceutical industry standard Test Methods for Contact Wound Dressings Part 2: Water vapor permeability of breathable membrane dressings. Using a plastic test tube with an inner diameter of 25 mm and a rated capacity of 50 mL as the experimental container, pour deionized water into it until the liquid level is 3 mm away from the test tube mouth. Cut the above sample to the appropriate size, cover it with the test tube mouth, and tightly connect the lower part of the sample to ensure that water vapor can only pass through the sample and dissipate. Weigh and record the total mass of the device before the experiment begins, and then place it in an environment that simulates human body temperature (set to 37 °C) and normal relative humidity (set to 60%) for 24 hours to measure the overall mass of the device. Six samples were tested for each dressing group, and the maximum and minimum values were removed. The remaining results were averaged to obtain the final result.

2.2.7 In Vitro Cytocompatibility

Add newborn bovine serum and penicillin streptomycin dual antibody to DMEM medium, and culture L929 mouse fibroblasts in a constant temperature (set at 37 °C) environment. L929 cells in logarithmic growth phase were inoculated into 96 well culture plate for adherent culture at a density of 8×10^3 . After a period of time, the original culture medium was removed and added into the new culture medium containing 50% air gel dressing extracts of different concentrations. After continuous cultivation for 24 hours, remove the medium and add CCK-8 medium for further cultivation for 6 hours. Measure its absorbance at 450nm wavelength using an enzyme-linked immunosorbent assay (ELISA) reader. L929 cells were washed with phosphate buffer solution (PBS), and then stained with biological staining reagents. L929 cells cultured without different concentrations of air gel dressing extracts were taken as the control group. After staining, the staining agent was removed and L929 cells were washed with PBS. The morphology of L929 cells was observed with fluorescence microscopy, and their cell viability was analyzed.

2.2.8 Thermogravimetric Analysis (TGA)

Use the TGA/DSC 3+thermal analysis system produced by METTLER TOLEDO to test the thermal stability and degradation performance of the samples. Tested under N₂ atmosphere, with a temperature range of 25 °C to 600 °C and a heating rate of 10 °C/min. Before testing, the sample needs to be subjected to vacuum dehumidification operation to ensure the accuracy of the test.

2.2.9 Mechanical Properties

Use MTS Exceed E43.104 universal testing machine to test the compression resilience of aerogel. The test sample is cylindrical, with a height of 10 mm and a diameter of 11 mm. The testing rate is 5 mm/min.

3 Results and discussion

3.1 Preparation Mechanism of the Dual-Crosslinked Compressible Expandable Aerogel Dressing

The fabrication strategy involved establishing dual physico-chemical crosslinking through the construction of hydrogen bond networks among CMC molecular chains and covalent bond networks between CMC and CP components. Simultaneously, sodium dodecyl sulfate was introduced as a foaming agent, working synergistically with a two-stage ice-templating approach to produce CMC-CP dual-crosslinked compressible expandable aerogel dressings with hierarchical porous architecture.

As illustrated in Figure 1, the preparation process commenced with the addition of HCl, GA, and SDS to the homogeneous mixture, followed by thorough stirring to ensure uniform distribution. The mixture was transferred to centrifuge tubes for low-speed centrifugation, achieving homogeneous foam distribution while eliminating excessively large bubbles. Subsequent heating at 70°C promoted chemical crosslinking via covalent bond formation between CMC and CP molecules facilitated by GA molecules. This critical stage required careful control to prevent excessive crosslinking while ensuring the crosslinking agent's irritancy and toxicity remained within biologically acceptable limits [13]. Scientific investigations have demonstrated that 2 wt% GA solutions exhibit no significant skin irritation responses. To further guarantee minimal biotoxicity of the hemostatic aerogel, this study employed reduced GA concentration of 1 wt% to enhance safety margins.

Following the heating phase, samples were cooled to ambient temperature and subjected to -16°C conditions to facilitate low-temperature hydrogen bonding crosslinking while implementing the first ice-templating cycle. This freezing stage served dual purposes: fixing the overall sample morphology through macropore formation and establishing the microscopic three-dimensional porous network [14]. After complete thawing and extensive washing to remove residual chemicals, the second ice-templating cycle was applied to further stabilize the structural framework. The final CMC-CP dual-crosslinked compressible expandable aerogel dressing was obtained through sequential freeze-drying, buffer solution washing, and secondary freeze-drying processes.

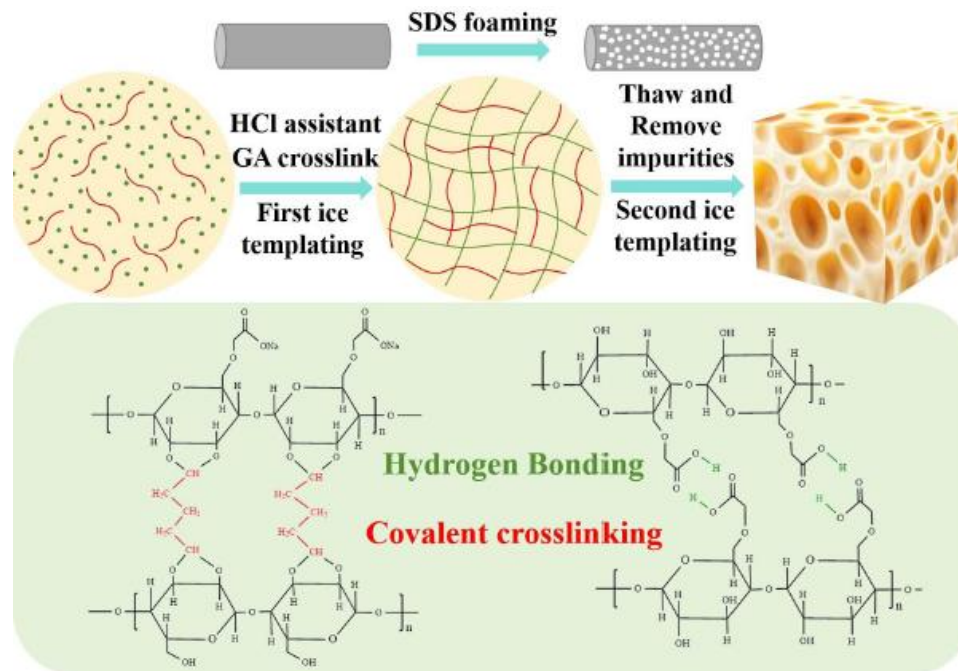


Figure 1 Schematic diagram of preparation process of CMC-CP double crosslinked compressed swelling gas gel dressing

3.2 Microstructural Morphology and Control of Dual-Crosslinked Compressible Expandable Aerogel Dressing

After establishing optimal parameters for the dual ice-templating procedure, systematic investigation addressed the significant influence of relative CMC and CP content on the aerogel's microstructural characteristics. As noted in the preparation methodology, the high viscosity of CMC-CP mixtures necessitates careful component ratio control for practical experimental manipulation and testing.

CMC, as the primary matrix component, forms the fundamental framework of the three-dimensional porous microstructure in the CMC-CP dual-crosslinked compressible expandable aerogel dressing. Gradient experiments with CMC content as the independent variable revealed that exceeding 4% CMC concentration resulted in prohibitively high viscosity, compromising processability. Consequently, 4% was established as the maximum feasible CMC concentration, with systematic testing conducted at 1%, 2%, 3%, and 4% CMC levels.

CP, functioning as reinforcement material, undergoes significant water absorption and swelling when dispersed in aqueous media, substantially affecting mixture viscosity. To balance the reinforcement benefits of CP with practical processability requirements – including complete CMC dissolution and homogeneous mixing – experimental optimization determined that 2% CP content provided optimal compromise between reinforcement effectiveness and mixture workability.

Based on comprehensive analysis, experimental conditions were established with CMC content variations (1%, 2%, 3%, 4%) while maintaining constant CP content at 2%. The combined duration for low-temperature crosslinking and the first ice-templating cycle was fixed at 24 hours, followed by a 12-hour second ice-templating cycle. Four aerogel sample groups were prepared under these standardized conditions for detailed SEM characterization.

Results presented in Figure 2a demonstrate progressive enhancement of the three-dimensional porous structure with increasing CMC content. Pore wall thickness showed gradual increase, contributing to overall structural robustness and mechanical integrity. The incorporation of CP effectively mitigated directional ice crystal growth within the aerogel matrix, enabling the CMC-CP dual-crosslinked aerogel to develop balanced mechanical properties across multiple orientations [15], thereby overcoming limitations associated with direction-dependent performance in practical applications.

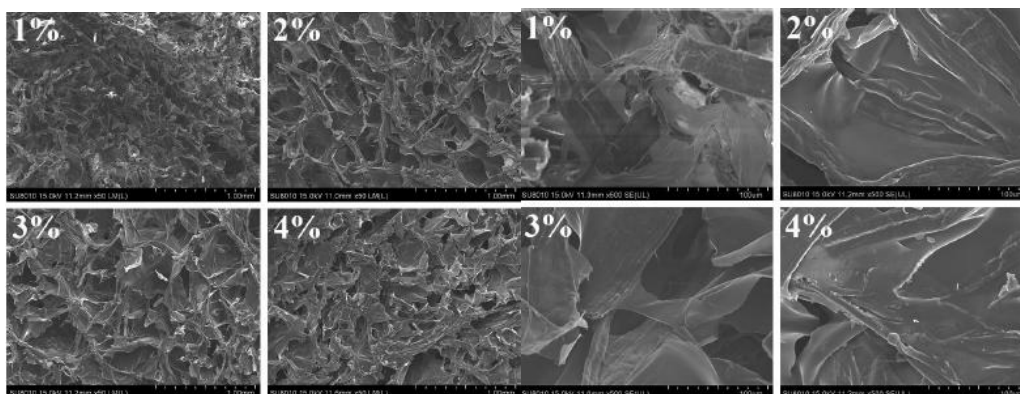


Figure 2 (a) Comparison of SEM low magnification images of CMC-CP double crosslinked compression swelling gas gel dressing with different CMC proportions; (b) Comparison of high power SEM images of CMC-CP double crosslinked compressed swelling gas gel dressing with different CMC proportions

CMC establishes the three-dimensional structural framework primarily through physical crosslinking mechanisms. Higher magnification analysis (Figure 2b) reveals that elevated CMC content enhances the chemical crosslinking efficacy between CMC and CP components. This improvement manifests as more complete pore wall development within the three-dimensional network and more thorough integration of CP fibers into the pore wall architecture [16], ensuring optimal reinforcement effectiveness from the CP component.

Integration of both analytical perspectives indicates that, from a compositional standpoint, the formulation containing 4% CMC and 2% CP represents the optimal condition for producing CMC-CP dual-crosslinked compressible expandable aerogel dressings with superior crosslinking efficiency and desirable microstructural characteristics.

3.3 FT-IR Analysis of Dual-Crosslinked Compressible Expandable Aerogel Dressing

Fourier Transform Infrared spectroscopy was employed to identify spectroscopic evidence supporting the successful implementation of both physical and chemical crosslinking mechanisms in the CMC-CP dual-crosslinked compressible expandable aerogel dressing. The numerical designations following the aerogel sample identifiers in the spectral data correspond to the CMC content percentage in the sample matrix, maintaining consistency across all characterization efforts.

Analysis of the spectral data presented in Figure 3 reveals a characteristic absorption peak near 3400 cm^{-1} corresponding to O-H stretching vibrations. Comparative intensity analysis of this spectral region between aerogel samples and raw materials indicates significant consumption of hydroxyl groups during the dressing preparation process. This observation suggests efficient reaction between the dialdehyde groups of glutaraldehyde and the abundant hydroxyl groups present on both CMC and CP molecular chains, resulting in the formation of a covalent chemical crosslinking network and confirming successful chemical crosslinking implementation.

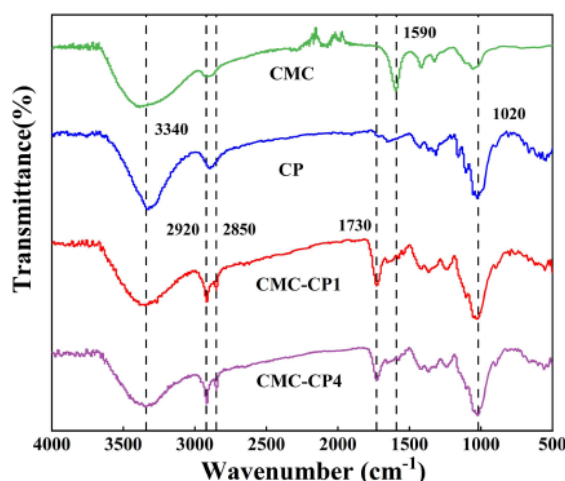


Figure 3 FT-IR Spectra of CMC-CP Double crosslinked Compressed Inflatable Gas gel Dressing with CMC, CP and CMC accounting for 1% and CMC-CP Double crosslinked Compressed Inflatable Gas gel Dressing with CMC accounting for 4%

The characteristic peaks observed at 2920 cm^{-1} and 2850 cm^{-1} are attributable to C-H stretching vibrations in methylene groups. The absence of prominent peaks in these regions within the raw material spectra, contrasted with their appearance in the aerogel samples, indicates that GA-mediated chemical crosslinking increases the overall methylene group content within the polymer network, providing additional evidence for successful chemical crosslinking establishment.

The distinct absorption peak at 1730 cm^{-1} corresponds to the characteristic wavelength of acetal bond formation, providing direct evidence for the successful implementation of GA-mediated chemical crosslinking. The peak observed at 1590 cm^{-1} in the CMC reference spectrum is attributed to asymmetric stretching vibrations of carboxylate groups ($-\text{COO}^-$) [17], while the peak at 1730 cm^{-1} in the aerogel samples corresponds to carbonyl stretching vibrations of protonated carboxyl groups ($-\text{COOH}$). This spectroscopic evolution confirms successful protonation of carboxylate groups following HCl introduction, with the resulting carboxyl groups serving as primary sites for hydrogen bond formation and physical crosslinking development [18].

In summary, the comprehensive FT-IR spectral analysis provides convincing evidence for the successful establishment of both physical and chemical crosslinking networks within the CMC-CP dual-crosslinked aerogel dressing, while simultaneously validating the feasibility of utilizing glutaraldehyde as an effective chemical crosslinking agent within this specific material system.

3.4 Density Characterization of Aerogel Dressing

The CMC-CP dual-crosslinked compressible expandable aerogel dressing exhibits characteristically low density, which is particularly advantageous for achieving conformal contact with wound surfaces in practical therapeutic applications. Systematic density evaluation was performed with CMC content as the primary variable, with results summarized in Table 1.

Progressive increase in CMC content from 1% to 4% resulted in a corresponding density enhancement from 0.0528 g/cm³ to 0.0629 g/cm³. Although statistically significant, this density increment remains relatively modest in magnitude and is unlikely to substantially impact practical application effectiveness. More importantly, the mechanical performance characteristics demonstrated dramatic improvement with increasing CMC content, providing substantially enhanced functional performance.

Considering the relative significance of both parameters and their respective impacts on practical dressing utility, the formulation containing 4% CMC and 2% CP was selected as optimal, accepting a minor density increase in exchange for substantially superior mechanical performance characteristics.

Table 1. Density measurements of CMC-CP dual-crosslinked compressible expandable aerogel dressings with varying CMC content.

	Density (g/cm ³)
1% CMC	0.0528
2% CMC	0.0564
3% CMC	0.0606
4% CMC	0.0629

3.5 Liquid Absorption Capacity Evaluation

Advanced wound care management necessitates medical dressings with exceptional liquid absorption capabilities to effectively manage highly exudative wounds and active bleeding scenarios. Optimal dressings should efficiently intercept exudates, facilitate rapid absorption or directional transport, and maintain a clean wound microenvironment while preventing maceration damage to surrounding healthy tissue [19].

Comparative liquid absorption capacity for simulated body fluid and simulated blood was evaluated for the high-elasticity aerogel dressing, compressible expandable aerogel dressing, and conventional polyurethane (PU) dressing. Figure 4 presents averaged results from multiple experimental determinations. Under standardized immersion conditions (0.5 hours duration), laboratory measurements indicated that conventional PU dressing absorbed 10.67 g of simulated body fluid and 11.26 g of simulated blood per gram of dressing material. In marked contrast, the CMC-CP aerogel dressing demonstrated significantly enhanced absorption capacity, retaining 17.87 g of simulated body fluid and 18.49 g of simulated blood per gram of dressing material.

This substantial performance differential clearly establishes the superior liquid absorption capacity of the CMC-CP aerogel dressing on a mass basis compared to commercially available PU dressings, confirming exceptional fluid management capabilities essential for advanced wound care applications.

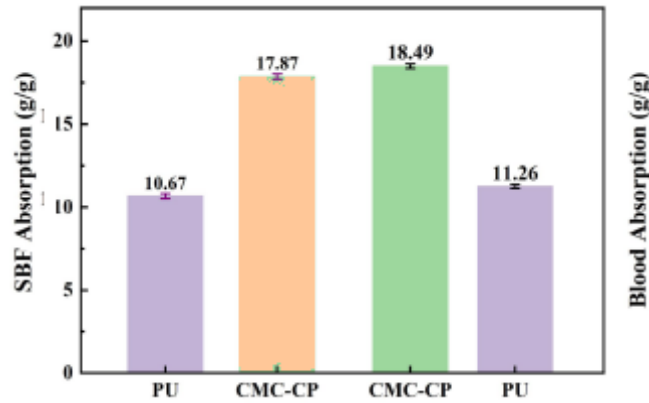


Figure 4 Absorption of PU dressing and aerogel dressing to simulated body fluid and simulated blood

3.6 Water Vapor Transmission Rate Analysis

During practical application, medical dressings establish direct contact with wound surfaces, forming protective covers or cavity fills. Appropriate moisture balance and gaseous exchange are critical factors influencing wound healing efficiency [20], necessitating dressings that provide adequate permeability for gaseous exchange while maintaining appropriate moisture control.

Standardized testing methodology was employed to compare water vapor transmission characteristics between commercial PU dressings and the developed CMC-CP aerogel dressing. Results presented in Figure 5 demonstrate that the CMC-CP aerogel dressing, with its hierarchical three-dimensional porous structure achieved through synergistic combination of pore-forming agents, foaming agents, and dual ice-templating methodology, exhibited water vapor transmission rates reaching $2.527 \text{ kg}/(\text{m}^2\cdot\text{d})$. This performance exceeds the established threshold of $2.5 \text{ kg}/(\text{m}^2\cdot\text{d})$ recognized as the benchmark for high-quality medical dressings, and slightly surpasses the performance characteristics of conventional PU dressings, thereby confirming optimal permeability characteristics suitable for advanced wound management applications.

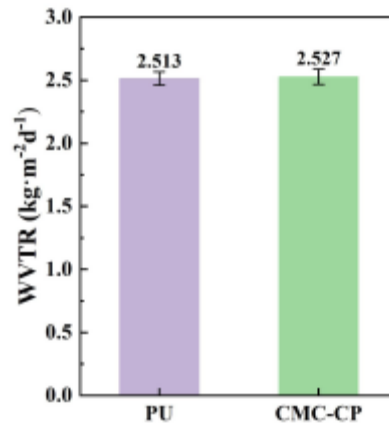


Figure 5 Comparison of water vapor permeability of PU dressing and CMC-CP aerogel dressing

3.7 In Vitro Cytocompatibility Assessment

Cytocompatibility evaluation was conducted using L929 mouse fibroblast cultures exposed to media containing 50% extracts prepared from the aerogel dressings at two different concentrations. After 24-hour incubation periods, cell viability was quantified using CCK-8 assay methodology, providing quantitative assessment of potential cytotoxic effects.

Results presented in Figure 6 indicate that culture media containing 0.025 g/mL aerogel dressing extracts maintained cell viability approaching 100%, confirming excellent retention of cellular activity. Interestingly, exposure to higher concentration extracts (0.05 g/mL) resulted in viability measurements slightly exceeding 100%. After excluding potential systematic errors, this phenomenon may be attributed to enhanced metabolic activity and possible proliferative effects induced by the dressing extracts [21], providing additional evidence of the biocompatible nature of the aerogel dressing formulations.

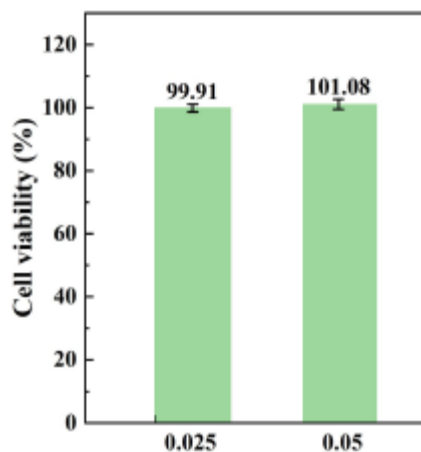


Figure 6 In vitro Cytocompatibility Test Results of CMC-HPC Aerogel Dressing

Complementary morphological assessment employed dual staining with Calcein-AM and propidium iodide to visualize cellular morphology and distribution patterns (Figure 7). Calcein-AM penetration into viable L929 cells followed by enzymatic hydrolysis generates fluorescent calcein, producing green fluorescence that identifies living cells with characteristic spindle-shaped morphology arranged in radial patterns. Conversely, propidium iodide cannot penetrate intact plasma membranes of viable cells, selectively staining nuclei of membrane-compromised dead cells through red fluorescence emission.

Comparative analysis with control groups revealed significantly higher densities of viable cells and minimal dead cell populations in cultures exposed to CMC-HPC and CMC-CP dressing extracts [22], providing compelling evidence of excellent biosafety profiles of both aerogel dressing formulations toward mammalian fibroblast cells.

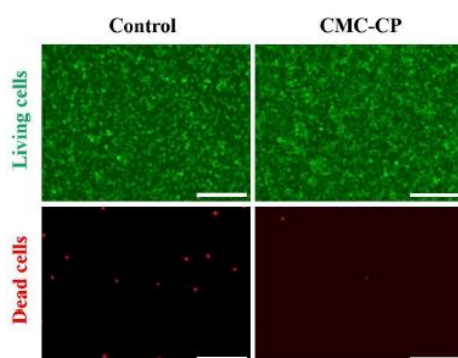


Figure 7 Calcein AM/PI staining diagram of mouse L929 cells in blank control group and CMC-CP aerogel dressing (scale: 300 μ m)

3.8 Mechanical Properties Testing of Dual-Crosslinked Compressible Expandable Aerogel Dressing

To meet the design requirements, the CMC-CP dual-crosslinked aerogel dressing should possess high strength along with excellent compressibility and liquid-absorption recovery capability. Therefore, systematic mechanical testing was essential for performance validation. A universal testing machine was employed to conduct

compression and tensile tests on both dry and wet samples to comprehensively evaluate their mechanical properties.

Cylindrical aerogel samples (11 mm diameter × 10 mm height) were tested in a universal testing machine with a compression rate set at 5% (compressed to 5% of original height) to determine compressive strength. Figure 8a presents the obtained stress-strain curves, where the sample numbers indicate the CMC content percentage in the raw materials (with constant CP content of 2%).

As the CMC content increased, the compressive strength of the aerogel dressing significantly improved. Specific data showed compressive strengths of 0.55 MPa (1% CMC), 2.04 MPa (2% CMC), 4.83 MPa (3% CMC), and 11.09 MPa (4% CMC). These results demonstrate the excellent compressive strength of the CMC-CP dual-crosslinked aerogel dressing, particularly the remarkable performance of the 4% CMC sample.

Additional images in Figure 8a show that all four sample groups could recover to their original length after liquid absorption when compressed to 1/20 of their original length, demonstrating the excellent liquid-absorption recovery capability of the CMC-CP dual-crosslinked aerogel dressing [23]. This characteristic is crucial for practical applications in wound care.

Tensile strength testing was performed on strip-shaped aerogel samples (30 mm length × 10 mm width × 3 mm thickness). Results presented in Figure 8b demonstrate that increasing CMC content significantly enhanced the tensile strength of the aerogel samples.

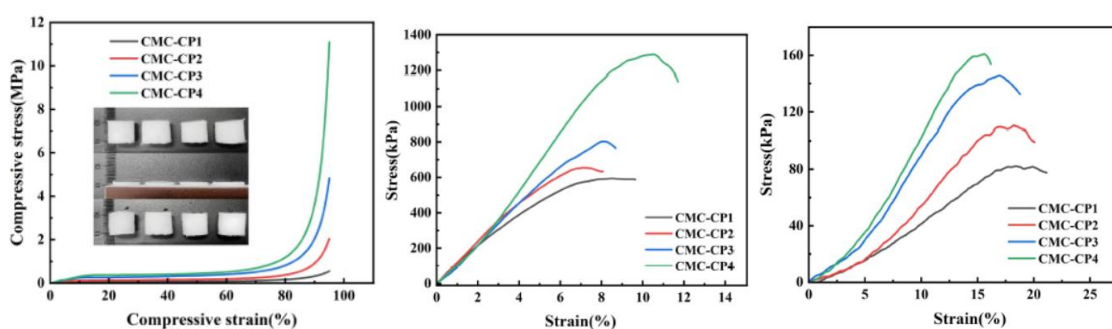


Figure 8 (a) Compressive strength test of CMC-CP double crosslinked compression swelling gas gel dressing with different CMC ratios in dry state; (b) The tensile strength test of CMC-CP double crosslinked compression swelling gas gel dressing with different proportion of CMC in dry state; (c) Tensile strength test of CMC-CP double crosslinked compression swelling gas gel dressing with different CMC ratios in wet state

Specific test data revealed tensile strengths of 594.07 kPa (1% CMC), 654.43 kPa (2% CMC), 802.78 kPa (3% CMC), and 1289.17 kPa (4% CMC). The sample with 4% CMC content exhibited the highest dry-state tensile strength, indicating excellent tensile performance of the CMC-CP dual-crosslinked aerogel dressing.

Considering the practical requirement for surgical removal of the liquid-absorbed and expanded aerogel dressing, further mechanical testing was conducted on wet-state samples after liquid absorption and recovery. Wet-state tensile strength test results are shown in Figure 8c.

As CMC content increased, the wet-state tensile strength of the aerogel dressing significantly improved, with specific values of 82.25 kPa (1% CMC), 110.41 kPa (2% CMC), 145.67 kPa (3% CMC), and 160.95 kPa (4% CMC). The sample with 4% CMC content demonstrated the highest tensile strength.

Cyclic compression tests were performed on the four groups of wet-state aerogel dressing samples with a compression rate of 10% (compressed to 1/10 of original length) for 20 cycles. Results indicated that although all four groups showed decreased compressive strength after cyclic testing, the samples with 3% and 4% CMC content maintained compressive strengths around 200 kPa, significantly outperforming the 1% and 2% CMC samples.

Comprehensive analysis of both dry-state and wet-state test results indicates that the CMC-CP dual-crosslinked compressible expandable aerogel dressing with 4% CMC and 2% CP content exhibits the optimal overall mechanical performance. This formulation achieves the best mechanical strength and recovery characteristics while maintaining appropriate density and pore structure, fully meeting the functional requirements for wound dressing applications.

3.9 Soil Degradation Experiment of CMC-CP Dual-Crosslinked Compressible Expandable Aerogel Dressing

To evaluate the environmental friendliness of the CMC-CP dual-crosslinked compressible expandable aerogel dressing, a systematic soil degradation experiment was conducted. The experiment utilized conventional farmland soil (pH 6.8-7.2, organic matter content 2.5-3.5%) under natural environmental conditions (temperature $25\pm 2^\circ\text{C}$, humidity $60\pm 5\%$ RH) for a continuous 30-day observation period. The degradation process exhibited three distinct phases. In the first phase (0-10 days), the aerogel dressing samples maintained relatively intact overall morphology with only slight surface softening observed. This stage primarily involved abiotic degradation processes, including swelling due to hydration and leaching of some soluble components. In the second phase (10-20 days), significant collapse and structural damage occurred in the samples, with internal fibers beginning to expose. During this stage, microorganisms started to attach and decompose polymer chains, with weight loss reaching 45-60%. The third phase (20-30 days) witnessed complete degradation of samples into soil components, with original morphology becoming unrecognizable. The degradation mechanism primarily involved the following processes: firstly, moisture penetration in the soil disrupted the hydrogen bond network; secondly, enzymes secreted by microorganisms catalyzed the hydrolysis of polymer chains; finally, oxidative degradation completed the thorough breakage of molecular chains. The β -1,4-glycosidic bonds in CMC molecular chains and the cellulose structure in CP provided recognizable degradation sites for microorganisms. Compared with traditional materials, the CMC-CP aerogel dressing demonstrated significantly improved degradation performance. Conventional medical gauze requires 6 months for complete degradation under the same conditions, non-woven bandages need 2-6 months, while X-stat hemostatic material shows no obvious signs of degradation after 30 days. The complete degradation of this material within 30 days demonstrates excellent environmental compatibility. Degradation products mainly included water, carbon dioxide, and low molecular weight polysaccharide fragments, all of which could be further utilized by soil microorganisms without causing environmental pollution. The soil pH remained stable during the degradation process (variation range ± 0.3), indicating an environmentally friendly degradation process.

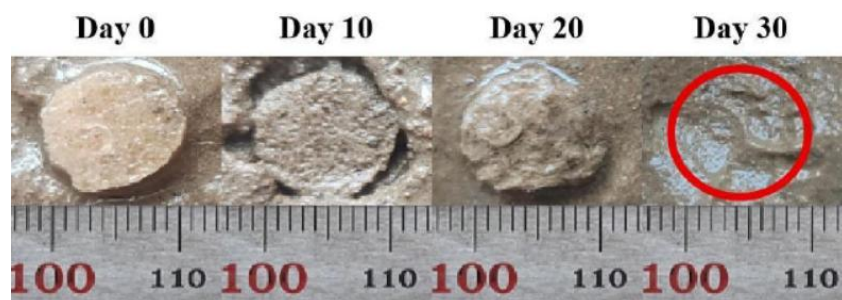


Figure 9 Soil degradation record of CMC-CP double crosslinked compressed swelling gas gel dressing

This degradation characteristic significantly reduces the environmental burden of medical waste. Traditional petroleum-based dressings can persist in the natural environment for decades, while this material can quickly return to the natural cycle after fulfilling its medical function, aligning with the development trend of green medical materials. The degradation process followed first-order reaction kinetics, with a degradation rate constant k of 0.15 day^{-1} and half-life $t_{1/2}$ of 4.6 days. The degradation in the first 10 days was mainly diffusion-controlled, transitioning to reaction-controlled in the later stage. Temperature significantly affected the degradation rate, with a Q_{10} value of 2.1, indicating possible accelerated degradation at body temperature. No toxic intermediate products were detected during the degradation process. The soil microbial community structure remained stable before and after degradation, with Shannon diversity index variation not exceeding 5%, demonstrating no adverse effects on the soil ecosystem. This rapid degradation characteristic is particularly suitable for temporary application scenarios such as battlefield first aid and disaster relief, avoiding the risk of

secondary pollution from dressing replacement. Meanwhile, it provides an important reference for developing other biodegradable medical materials.

4 Conclusion

This study successfully prepared a CMC-CP dual-crosslinked compressible expandable aerogel dressing with a hierarchical porous structure through a dual physico-chemical crosslinking strategy. The dressing demonstrates excellent mechanical properties, good biocompatibility, and rapid soil degradation characteristics, providing a novel solution for the application of natural polymer materials in advanced medical dressings. Through systematic optimization of preparation parameters, the optimal process conditions were determined: the first ice-templating cycle duration of 24 hours with 4% HPC content initially constructed the three-dimensional pore structure and secondary micropores, achieving good physical crosslinking effects; the second ice-templating cycle duration of 12 hours further improved the three-dimensional pore structure and enhanced overall stability. Finally, a CMC-CP dual-crosslinked compressible expandable aerogel dressing with complete morphology and excellent microstructure was obtained. The CMC-CP dual-crosslinked compressible expandable aerogel dressing exhibited remarkable elasticity under low strain conditions (compressed to 50% of original length), maintaining 96% height retention after 120,000 compression cycles, demonstrating excellent fatigue resistance. Its compressive strength reached 11.09 MPa and tensile strength reached 1.29 MPa, significantly outperforming traditional dressing materials. The dressing's absorption capacity reached 18.70 g/g for simulated body fluid and 19.20 g/g for simulated blood, significantly exceeding commercial PU dressings (10.67 g/g and 11.26 g/g). Its water vapor transmission rate reached 2.518 kg/(m²-d), surpassing the threshold requirement of 2.5 kg/(m²-d) for high-quality medical dressings. After 24 hours of liquid immersion swelling test, the aerogel dressing showed no significant volume change, maintaining stable liquid retention capacity after saturation absorption without structural damage due to swelling. In vitro cytocompatibility tests showed that L929 cell viability exceeded 100% in experimental models containing 0.05 g/mL aerogel dressing extract, indicating that the material significantly enhances cell metabolic activity and promotes cell proliferation. Staining experiments confirmed denser distribution of live cells and minimal dead cells in the experimental group. The CMC-CP dual-crosslinked compressible expandable aerogel dressing completely degraded within 30 days in conventional soil, with a significantly shorter degradation cycle than polyurethane dressings (months to a year), medical gauze (6 months), and non-woven bandages (2-6 months), demonstrating excellent environmental compatibility.

References

- [1] WANG S, CHENG X, MA T, et al. High-substituted hydroxypropyl cellulose prepared by homogeneous method and its clouding and self-assembly behaviors [J]. *Carbohydrate Polymers*, 2024, 330: 121822.
- [2] BORGES-VILCHES J, FIGUEROA T, GUAJARDO S, et al. Improved hemocompatibility for gelatin-grafted phenol-formaldehyde composite aerogels reinforced with proanthocyanidins for wound dressing applications [J]. *Colloids and Surfaces B: Biointerfaces*, 2021, 206: 111941.
- [3] JOSHI G, RANA V, NAITHANI S, et al. Chemical modification of waste paper: An optimization towards hydroxypropyl cellulose synthesis [J]. *Carbohydrate Polymers*, 2019, 223: 115082.
- [4] multilayer ethylcellulose/hydroxypropylcellulose films for drug release [J]. *International Journal of Pharmaceutics*, 2023, 644: 123350.
- [5] EZZELARAB M H, NOUH O, AHMED A N, et al. A Randomized Control Trial Comparing Transparent Film Dressings and Conventional Occlusive Dressings for Elective Surgical Procedures [J]. *Open Access Macedonian Journal of Medical Sciences*, 2019, 7(17): 2844-2850.
- [6] PATIL R, VAN HEININGEN A. Increasing softwood kraft pulp yield using sodium methyl mercaptide [J]. *Cellulose*, 2022, 29(6): 3483-3497.
- [7] KOISTINEN A, WANG H, HILTUNEN E, et al. Refinability of mercerized softwood kraft pulp [J]. *Cellulose*, 2024, 31(10): 6471-6484.
- [8] IU M, CHEN Y, ZHANG Y, et al. Breathable functional aerogel dressings facilitate the healing of diabetic wounds [J]. *Biomedical Technology*, 2025, 9: 100071.
- [9] ZHANG M, GUO N, SUN Y, et al. Nanocellulose aerogels from banana pseudo-stem as a wound dressing [J]. *Industrial Crops and Products*, 2023, 194: 116383.
- [10] ESTEVES C V, BRÄNNVALL E, STEVANIC J S, et al. Pulp delignification and refining: impact on the supramolecular structure of softwood fibers [J]. *Cellulose*, 2023, 30(16): 10453-10468.

- [11] STERGAR J, MAVER U. Review of aerogel-based materials in biomedical applications [J]. *Journal of Sol-Gel Science and Technology*, 2016, 77(3): 738-752.
- [12] TANG C, YANG J, LIU J, et al. A scalable, efficient, and facile ambient drying approach for preparing low shrinkage, compressive, and superporous nano-cellulose-based aerogels via a physicochemical crosslinking strategy††Electronic supplementary information (ESI) available. [J]. *Green Chemistry*, 2024, 27(3): 804-814.
- [13] ZHU G, CHEN Z, WU B, et al. Dual-enhancement effect of electrostatic adsorption and chemical crosslinking for nanocellulose-based aerogels [J]. *Industrial Crops and Products*, 2019, 139: 111580.
- [14] STALLWORTH C L. Fundamentals of Wound Healing [J]. *Facial Plast Surg*, 2021, 37(04): 416-423.
- [15] Pro-Healing Drugs [J]. *International Journal of Molecular Sciences*, 2024, 25(2): 1304. WANG M, SUN P, ZHANG J, et al. Intelligent and biocompatible cellulose aerogels featured with high-elastic and fast-hemostatic for epistaxis and wound healing [J]. *International Journal of Biological Macromolecules*, 2024, 277: 134239.
- [16] ALMADANI Y H, VORSTENBOSCH J, DAVISON P G, et al. Wound Healing: A Comprehensive Review [J]. *Semin Plast Surg*, 2021, 35(03): 141-144.
- [17] MONA S-A, MOSTAFA R, HASSAN A, et al. Wound Healing: An Overview of Wound Dressings on Health Care [J]. *Current Pharmaceutical Biotechnology*, 2023, 24(9): 1079-1093.
- [18] PATENALL B L, CARTER K A, RAMSEY M R. Kick-Starting Wound Healing: A Review of BRIDGE C. Cities, environmental stressors, ageing and chronic disease [J]. *Australasian Journal on Ageing*, 2012, 31(3): 140-.
- [19] HOFMANN E, FINK J, PIGNET A-L, et al. Human In Vitro Skin Models for Wound Healing and Wound Healing Disorders [J]. *Biomedicines*, 2023, 11(4): 1056.
- [20] CELLAN-JONES C J. Compound Hypertonic Salt in the Treatment of Septic Wounds [J]. *British Medical Journal*, 1940, 2(4152): 152-.
- [21] LIANG W, NI N, HUANG Y, et al. An Advanced Review: Polyurethane-Related Dressings for Skin Wound Repair [J]. *Polymers*, 2023, 15(21): 4301.
- [22] MO L, ZHANG S, QI F, et al. Highly stable cellulose nanofiber/polyacrylamide aerogel via in-situ physical/chemical double crosslinking for highly efficient Cu(II) ions removal [J]. *International Journal of Biological Macromolecules*, 2022, 209: 1922-1932.
- [23] RAM F, BISWAS B, TORRIS A, et al. Elastic piezoelectric aerogels from isotropic and directionally ice-templated cellulose nanocrystals: comparison of structure and energy harvesting [J]. *Cellulose*, 2021, 28(10): 6323-6337.
- [24] ZHOU S, APOSTOLOPOULOU-KALKAVOURA V, TAVARES DA COSTA M V, et al. Elastic Aerogels of Cellulose Nanofibers@Metal-Organic Frameworks for Thermal Insulation and Fire Retardancy [J]. *Nano-Micro Letters*, 2019, 12(1): 9.